Multi-fidelity Simulation Modelling in Optimization of a Submarine Propulsion System

Arturo Molina-Cristóbal, Patrick R. Palmer, Benjamin A. Skinner, Geoffrey T. Parks
Engineering Design Centre (EDC), Department of Engineering
University of Cambridge, Cambridge, England
Email: am664@cam.ac.uk, prp@cam.ac.uk, bas24@cam.ac.uk, gtp10@cam.ac.uk

***Abstract*— An inherent trade-off exists in simulation model development and use: a trade-off between the level of detail simulated and the simulation model's computational cost. It is often desirable to simulate a high level of detail to a high degree of accuracy. However, due to the nature of design optimization, which requires a large number of design evaluations, the application of such simulation models can be prohibitively expensive.**

This paper presents an optimization framework consisting of a series hybrid optimization algorithm, in which a global search optimizes a submarine propulsion system using low-fidelity models and, in order to refine the results, a local search is used with high-fidelity models.

I. Introduction

In this paper the optimization of a submarine propulsion system is tackled, see Fig. 1. The optimization has multiple objectives, such as the maximization of the efficiency of each component (propeller, gear box, electric motor, AC generator, steam turbine) while minimizing the total energy consumption and peak motor power across a range of velocity profiles or scenarios. By setting velocity profiles *a priori* we can go beyond design-point performance-based optimization, where we design for a single operating point, and instead design for a range of operating conditions. Four mission scenarios (Escort, Reconnaissance, Combat, Deterrence) are used to represent typical operating conditions a submarine experiences at sea. Mission scenarios were created in consultation with a leading company in the UK defense sector.

The detailed simulation of submarine propulsion systems is computationally expensive, due to its multi-disciplinary nature and the number of different devices simulated within the system, as shown in Fig. 1. The optimization process requires many simulations runs, so reducing the computational cost is highly desirable.

One approach to reducing computational cost while maintaining a high level of detail and accuracy in the final design is to employ multi-fidelity simulation, which combines the use of both "cheap" low-fidelity models, such as efficiency maps, and higher-fidelity models, which are more computationally expensive due to the nature of the numerical methods used to solve the equations which represent the model. An issue that arises in this approach is the question of when to switch from global (low-fidelity) to local (higher-fidelity) optimization in order to minimize the overall computational cost without reducing the quality of the final design. This question is addressed in this paper. The higher-fidelity model and the series hybrid optimization method are presented, and complete results are presented in Section V.

II. Multi-fidelity Simulation Modelling

Multi-fidelity simulation modelling has received considerable attention over the past few years, especially in the computational fluid dynamics (CFD) and finite element analysis (FEA) communities where simulation costs are very high. Examples of multi-fidelity modelling in the CFD community include airfoil design [2], [3], [4] and aircraft design [5]; Hutchinson et al. [6] linked a high-fidelity CFD aerodynamic model with a low-fidelity simple algebraic model in the optimization of a high speed civil transport wing. FEA applications include structural synthesis and design [7], [8] and multi-phase material design [9]. Haftka [10] uses a high-fidelity FEA model with a crude low-fidelity FEA model to optimize structural cross-sections to maximize a structure's buckling load. In each case low-fidelity models are used to approximate the behaviour of the high-fidelity models for use during optimization, resulting in significant reductions in optimization time compared to the use of high-fidelity CFD and FEA models. This approach can also be applied to other simulation environments to reduce the computational cost of the optimization process.

Low-fidelity models can be roughly divided into three categories [4]: *data fitting*, typically using interpolation or regression of the high-fidelity model [7], for example Kriging [9], [11], [12] and Knowledge Based Neural Networks [13], [2]; *reduced-order models*, derived using techniques such as modal analysis [8] and proper orthogonal decomposition [14]; and *multi-fidelity* (also known as variable-fidelity, or variable complexity models) [3], [15]. In the latter case, a physics-based model of reduced computational cost (and usually of lower accuracy) is used in conjunction with the high-fidelity model. The lower-fidelity hierarchical model can be based on the same physical model as the higher-fidelity model but with a lower tolerance, a coarser grid or step size, or it can be a simpler engineering model. The following sections describe such choices made for the various parts of a multi-disciplinary submarine propulsion system model. Practical choices must be made to allow the multi-objective optimization to yield useful detail in an acceptable time.

978-1-4244-8218-4/10/$26.00 ©2010 IEEE

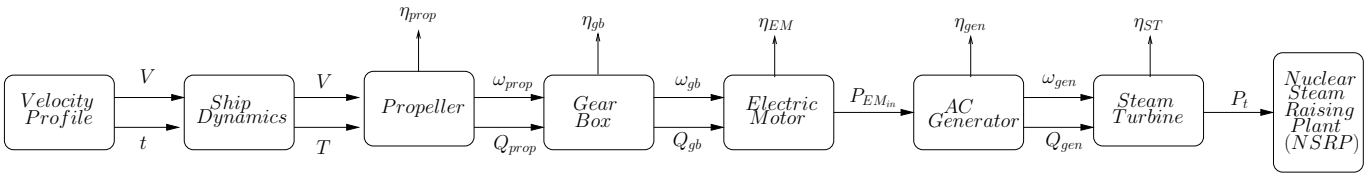

Fig. 1. Information flow within the propulsion system simulation.

III. Approach

In [1] Skinner et al. introduced a method for performing a conceptual comparison study of different submarine propulsion systems and an approach to generate a set of optimal preliminary designs. Four topologies were considered. In this paper, for reasons of space, only one topology, the *Electric Drive*, will be considered.

For a conceptual comparison study it is desirable to have relatively inexpensive simulation models that help facilitate global search across a very broad design space. The use of higher-fidelity simulation models, in this case, would be prohibitively expensive. Once the design landscape has been mapped and an impression gained of the performance of each concept, it is then desirable to explore the selected concept's design space in more detail. This is where higher-fidelity simulation models can be utilised. Here, the quasi-static simulation models introduced in [1] are used with a global optimization method, the multi-objective Genetic Algorithm (MOGA) as detailed previously in [16], and higher-fidelity simulation models are used with a multi-objective Tabu Search (MOTS) algorithm [17]. The MOTS method is chosen for its local search attributes, which allow it to explore the Pareto front locally, while retaining the multi-objective nature of the problem. Thus the conceptual, preliminary and detailed design phases can be combined in a single optimization process.

The best point at which to switch model fidelity must be decided. The change in optimization method also requires that the number of designs carried forward is limited. For research purposes, the quality of the developing Pareto front in each run can be estimated by comparing the results against the Pareto front produced using the archive of results as a reference set.

In the sections that follow, higher-fidelity simulation models are introduced for a number of system components (propeller, electric motor, steam turbine), and the low-fidelity simulation models are calibrated against the new higher-fidelity models to give a set of multi-fidelity simulation models. A schematic of the information flow within the propulsion simulation model is presented in Fig. 1. Inverse simulation is employed.

A. Design Space Mapping

According to Robinson et al. [4] multi-fidelity optimization methods had, until that time (2006), been applicable only to models where both the low-fidelity $f(x_L)$ and high-fidelity models $g(x_H)$ are defined over the same design space, i.e. $x_L = x_H$. Difficulties arise when the two design spaces differ, in both dimensionality and content, i.e. $x_L \neq x_H$. For example, in aircraft design a high-fidelity CFD model may require a detailed description of the aircraft geometry, while the low-fidelity model may only require higher-level design variables, such as wing area, aspect ratio and sweep.

TABLE I
Design variables: Low-fidelity and higher-fidelity design space for propeller, electric motor, steam turbine and AC generator

Model	Decision Variables
Propeller	d_{prop}, propeller diameter
	A_E/A_O, propeller blade-area ratio
	P/D, pitch-diameter ratio
	Z, number of propeller blades
Electric Motor	P_{EM}, maximum power
Steam Turbine	L_{ST}, steam turbine power
	ϵ_{boiler}, boiler superheat factor
	p_{boiler}, boiler pressure
	$p_{condenser}$, condenser pressure
AC Generator	L_{ACgen}, AC generator rated power

The design space of the submarine propulsion multi-fidelity simulation models employed in the following sections are defined over the same design space dimensionality, to avoid difficulties in mapping or inappropriate constraining of the design. Nonetheless, the high-fidelity design space is evaluated in more detail than its low-fidelity equivalent. Details of the design variables used are given in Table I. Mapping between low and high fidelity is achieved by inserting the low-fidelity design variables directly into the higher-fidelity design space, thus allowing the optimization to refine the values.

The low-fidelity models are derived and calibrated in the form of efficiency maps, for the steam turbine, f_{ST}, and propeller, f_{prop}, with data coming from the higher-fidelity models. Four design parameters are considered in each case:

$$\eta_{prop} = f_{prop}(d_{prop}, A_E/A_O, P/D, Z)$$
$$\eta_{ST} = f_{ST}(L_{ST}, \epsilon_{boiler}, p_{boiler}, p_{condenser}) \quad (1)$$

The efficiency maps are lookup tables in four dimensions with 20 points spread linearly, and simple linear interpolations are performed. An efficiency map for the induction motor was not necessary, since the well-known per-phase equivalent circuit model has approximately the same computational cost as an efficiency map with interpolation.

No empirical design space mapping algorithms are therefore needed, nor any elaborate model management strategy to facilitate the mapping of the design space. This is beneficial to

both the overall computational cost of the optimization process and the complexity of its implementation.

B. Objective Functions

Six objective functions are considered here with the design variables detailed in Table I. The six objective functions (2) are evaluated for four velocity profiles or mission scenarios. Constraints are added to check the allowability of the size of the electric motor, generator and steam turbine and the dryness of the steam turbine cycle, giving a total of 24 objectives and 5 constraints. The optimization problem is thus clearly multi-objective, and any attempt to reduce the number of objectives would not be appropriate for a multi-role submarine.

$$\begin{array}{lll} \text{maximize} & F_1 = \eta_{prop}, & \text{propeller efficiency} \\ \text{maximize} & F_2 = \eta_{EM}, & \text{electric motor efficiency} \\ \text{maximize} & F_3 = \eta_{ST}, & \text{steam turbine efficiency} \\ \text{maximize} & F_4 = \eta_{gen}, & \text{AC generator efficiency} \\ \text{minimize} & F_5 = P_{EM}, & \text{peak electric motor power} \\ \text{minimize} & F_6 = P_{total}, & \text{total energy consumption} \end{array} \tag{2}$$

C. The Hybrid Optimization Method

MOTS uses an effective and popular local search method known as the Hooke and Jeeves (H&J) direct search method [18]. This method combines a deterministic exploratory search phase with a pattern search phase that embodies some of the characteristics of more sophisticated gradient-based methods. MOTS couples the H&J local search algorithm with a *short term memory* to archive recently visited points, which are "tabu" – the search is not allowed to revisit these points, a *medium term memory*, to archive the explored Pareto front, and an *intensification memory* (IM) which contains unexplored Pareto front points. MOTS can also use a *long term memory*, which facilitates diversification (global search). This is not used here because global search is performed by MOGA using low-fidelity models. Thus MOTS is combined with MOGA to form a hybrid optimization framework.

The hybridization allows the two algorithms to function in synergy, capitalising on MOGA's ability to locate promising regions in the search space and MOTS' ability to refine designs through local search. The reciprocal advantages and disadvantages of both search methods result in a hybrid optimization algorithm that is simultaneously global and precise, facilitating the generation of refined design solutions from a large and complex design space.

The hybrid optimization process follows Fig. 2:

1) Randomly create a population of initial designs.
2) MOGA performs global search optimization by evaluation, selection, crossover and mutation for a number of generations.
3) The number of generations for which MOGA is run can be varied and terminates at the switch point,
4) 300 designs are randomly chosen from the Pareto front produced by MOGA.
5) The selected designs are re-evaluated in the higher-fidelity design space and their objective function values archived.
6) Local search is performed on each selected design using MOTS, with the Pareto front produced by MOGA used as the initial IM.
7) Stop when the Pareto front shows no sign of change or when a maximum number of cycles has been executed.

Each process within the optimization framework is integrated into a single executable script that is run within Matlab. This allows the effect of the switch point to be examined.

IV. Higher-Fidelity Simulation Models

A. Propeller Simulation Model

In [1] an inverse propeller simulation model was introduced based on polynomial regression analysis of the Wageningen B-screw series of propellers. This model is extended to include variations in the propeller pitch-diameter ratio P/D, propeller blade-area ratio A_E/A_O, and the number of propeller blades Z. The values of the non-dimensional thrust coefficient K_T and torque coefficient K_Q are now expressed in terms of polynomials, which are derived from multiple regression analysis [19]:

$$K_T = \sum_{s,t,u,v} C_{T_{s,t,u,v}} (J)^s (P/D)^t (A_E/A_O)^u Z^v \tag{3}$$

$$K_Q = \sum_{s,t,u,v} C_{Q_{s,t,u,v}} (J)^s (P/D)^t (A_E/A_O)^u Z^v \tag{4}$$

where J is the advance factor and the polynomial coefficients $C_{T_{s,t,u,v}}$ and $C_{Q_{s,t,u,v}}$ and the terms s, t, u, v are given in [19].

The derived regression polynomials can be used to evaluate the K_T and K_Q for the following design variable ranges:

$$2 \leq Z \leq 7, \tag{5}$$

$$0.5 \leq P/D \leq 1.40, \tag{6}$$

$$0.30 \leq A_E/A_O \leq 1.05. \tag{7}$$

It should be noted, however, that at the extremes of the above ranges the results are slightly erroneous due to limitations of the regression analysis [19]. Efficiency values at these extremes must therefore be treated with caution.

B. Electric Motor Drive System Simulation Model

Rather than use an efficiency map to simulate the combined efficiency of the induction motor and its converter [1], a higher-fidelity model was derived and used in all cases. Based on the conventional equivalent circuit technique, it allows the drive electronics to impose full flux operation (a constant ratio of voltage to frequency), with a small slip. This approach is efficient in simulation as it also allows the 'full load torque' constraint to be applied across the four scenarios and correct matching to the propeller load and converter.

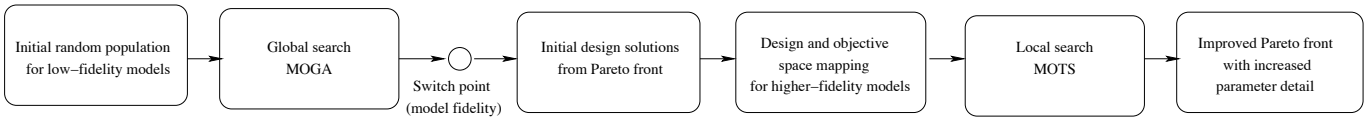

Fig. 2. Hybrid optimization framework.

The useful mechanical power at the shaft or the input power required at the shaft is:

$$P_{shaft} = \frac{\omega_r(t) Q_r(t)}{P_{shaft_{rated}}} \tag{8}$$

where $\omega_r(t)$ and $Q_r(t)$ are the input variable rotor speed and torque respectively, and $P_{shaft_{rated}}$ is the maximum power provided. P_{shaft} can be calculated from power balance considerations [20] as:

$$\begin{aligned} P_{shaft} P_{shaft_{pu_{rated}}} &= P_{em_{pu}} - P_{fw_{pu}} N_r^m \\ &\quad - P_{stray_{pu}} N_r^n \end{aligned} \tag{9}$$

where $P_{fw_{pu}}$ and $P_{stray_{pu}}$ are the friction + windage and stray losses at full load, respectively, and $P_{em_{pu}}$ is the electromechanical power.

Efficiency: Using the inverse model, the stator current, stator voltage, power factor and the input power, $P_{EM_{in_{pu}}}$, are found. The efficiency, η_{EM}, is then:

$$\eta_{EM} = \frac{P_{shaft_{pu_{rated}}}}{P_{EM_{in_{pu}}}} \tag{10}$$

The electric motor simulation parameter values were provided by Converteam Ltd., through a confidentiality agreement [20]. The simulation model results have been verified against benchmark test results provided by Converteam Ltd. and the simulation model is deemed representative of a typical MW marine electric motor. The motor is scaled for each design solution and the overall efficiency obtained as described. With this approach, the motor is operated at all times within its rated full load torque. The converter efficiency is applied as a fixed 98% value.

C. Steam Turbine Cycle Simulation Model

In this section an inverse simulation model is presented that covers the complete nuclear propulsion system, from the nuclear steam-raising plant, feed pump and condenser, through to the dryness of the steam turbine exhaust. The nuclear propulsion plant consists of two basic systems: a primary system and a secondary system.

The simulation model presented here simulates the secondary system. This system consists of a boiler, engine throttle, steam turbine, condenser and feed pump. The system is split into 5 sections or $states$ and the steam cycle simulated here is based on a non-ideal Rankine cycle that takes into account the non-isentropic inefficiencies of the steam turbine, η_{ST}, and feed pump, η_{pump}, and also the action of the engine throttle. The efficiency of the complete nuclear propulsion steam turbine cycle, $\eta_{STcycle}$, can then be calculated.

The modelling assumptions made place limitations on the model's range of validity. By assuming the first row of the steam turbine remains choked across all operating conditions, the model becomes unreliable when propulsive loads are very low. When propulsive loads are low the pressure drop across the throttle is large and the difference between the steam turbine inlet and outlet pressures reduces to an extent that choked operation cannot be sustained. Consequently the change in enthalpy across the steam turbine is underestimated, as is the corresponding low-load system efficiency. Therefore the results from the simulation model at low propulsive loads must be treated with caution.

Verification of the simulation model against real-life test data for nuclear submarine propulsion is difficult as test data is not readily available. However, a comparison has been made against simulation models provided by DSTL and Mathworks.

V. Results

The output of the multi-objective optimization problem (2) is a set of solutions approximating the Pareto-optimal set. Here, the end result of the optimization is a set of ∼1000 optimal designs for the 24 objectives, as shown in Fig 3. Only four of the 15 meaningful pairings of objectives are shown. The plot of motor size with propeller efficiency (top left), as expected, does not show any conflict. Nonetheless, each point is Pareto-optimal elsewhere in the 15 pairings. The plot of energy consumption with propeller efficiency (top right) shows that a high efficiency propeller is not necessarily an overarching design consideration, and a high efficiency propeller does not uniquely define a low energy consumption.

To establish the performance of the hybrid optimization method, some measure of progress is required. The unary epsilon indicator, ε, was proposed by Zitzler et al. [21] and makes direct use of the principle of Pareto-dominance, having a direct relationship with the formation of the Pareto front. The epsilon indicator is a measure of the smallest distance one would need to translate every point in a set so that it dominates a reference set.

To create a reference set of results, MOGA with higher-fidelity models was run five times for 100 generations with a population of 100 individuals, resulting in 10,000 design evaluations in each run. The reference set is then the Pareto-optimal set produced by combining the 5 Pareto-optimal sets obtained [21]. The local search carried out with MOTS in the hybrid optimizer was also run for 10,000 evaluations for comparison purposes following 100 generations of MOGA with low-fidelity models (not shown). Fig. 4 shows the performance of the two algorithms, with five similar runs of each.

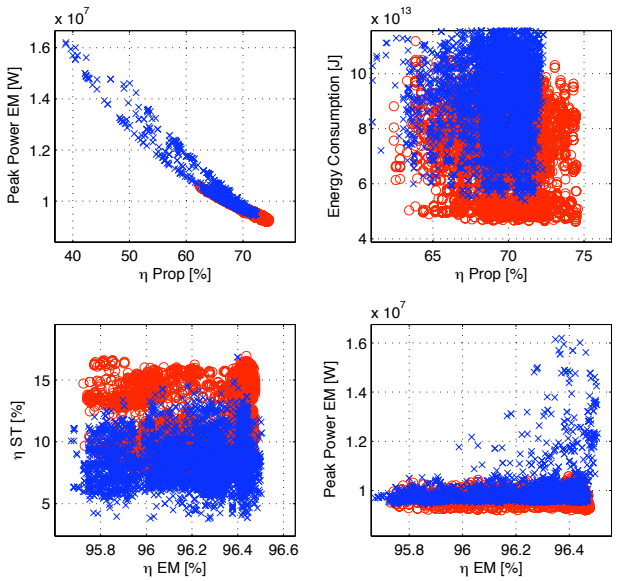

Fig. 3. Results from the multi-objective optimization: a subset of Pareto-front projections for the Escort scenario, where red circles are the outcome of a single run of the hybrid algorithm and the blue x's are the outcome of a single MOGA run with higher-fidelity models.

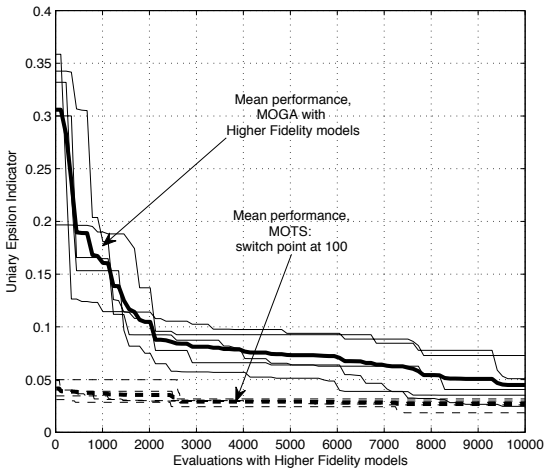

Fig. 4. Epsilon indicator performance: comparison of 5 runs for each case. Solid lines: MOGA with higher-fidelity models; dashed lines: hybrid optimization.

It can be seen that the performance of the hybrid optimizer with MOTS is good from the start and less varied than MOGA with higher-fidelity models. It is worth noting that in most cases the low-fidelity MOGA used in the hybrid optimization is producing as good results as MOGA with higher-fidelity models, at much lower cost. Within the 5 MOGA runs with higher-fidelity models, quite varied performance can be observed: one run converges fast (in around 2000 evaluations) from a poor start, whereas another has a good start but struggles to converge to a small epsilon value.

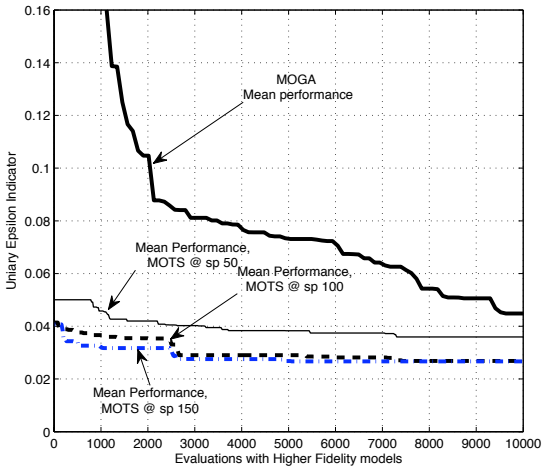

Fig. 5. Epsilon indicator performance: comparison of means of 5 runs.

An investigation of the effect of switch point from low fidelity/global search to higher fidelity/local search was carried out. Results are presented in Fig. 5 for sp values of 50, 100 and 150, showing the mean performance of 5 runs for each case. The starting point for MOTS with $sp = 50$ is worst, as expected, and the local search does not recover the deficit. The performance for $sp = 100$ and $sp = 150$ is similar, with the latter making slightly more rapid progress.

The computational cost of executing the complete optimization framework is studied in Table II. The computation was carried out on a 2.40GHz two quad-core processor workstation with 4GB of RAM, with the evaluations parallelized over the 8 cores. A single evaluation of a low-fidelity model takes $\sim$4 seconds and a higher-fidelity model takes $\sim$60 seconds, and the total execution time for a single optimization run is presented. Based on the observation that MOTS converges in around half the evaluations required by MOGA with higher-fidelity models, the computational cost saving is also approximately half, as the time spent with MOGA in the hybrid optimization is a small fraction of the total time.

VI. Discussion

From these results it can be proposed that the hybrid simulation approach is a practical solution. However, preparation of the low-fidelity models has a significant effect on the outcome. Low-fidelity models could be developed by fixing some parameter values, simplifying the equations and making use of synthetic models or maps. With low-fidelity models, where the design is in the conceptual design phase, reliable fixed values may be adopted. However, a choice of typical fixed values is unlikely to lead to successfully optimized higher-fidelity models: careful consideration of the mapping to the higher-fidelity models is required. Here, using all the decision variables to develop efficiency maps leads to good performance.

These results also show that a physically defined simplified

TABLE II
COMPUTATIONAL COST

Optimizer	Low-fidelity model evaluations	Mapping with HF model evaluations	Execution time [hr] with low-fidelity	Higher-fidelity model evaluations	Execution time [hr] with higher-fidelity	Total execution time [hr]
MOGA	none	none	-	10000	20.8333	20.8333
Hybrid sp @ 50	5000	300	1.3194	5000	10.4167	11.7361
Hybrid sp @ 100	10000	300	2.0139	5000	10.4167	12.4306
Hybrid sp @ 150	15000	300	2.7083	5000	10.4167	13.1250

model may perform better than a performance map, as the map requires interpolation and scaling to find values. A synthetic model capturing basic behaviour also requires evaluations and scaling. Here the induction motor has a well-understood equivalent circuit model that performs well when suitable scaling is applied.

The switch point study shows that increasing sp improves the optimization at a relatively low computational cost, Table II. However, the linear interpolation between points in the maps of the low-fidelity propeller model means there is inherent error in low-fidelity designs. This source of error is removed once the switch over has taken place, increasing confidence in the optimized designs produced.

VII. CONCLUSIONS

The combination of MOGA for the initial investigation of the designs followed by a MOTS-based local search resolves the issues of slow MOGA convergence and MOTS's lack of speed. A long low-fidelity run is preferred. The induction motor model used in the low-fidelity modelling is an example of a multi-fidelity model and was found to work as well as an efficiency map model whist retaining a great deal of physical meaning, which allows bounds on the behaviour, scaling and an operating regime to be applied appropriately. This work shows that the initial low-fidelity run should have the same list of design parameters as the high-fidelity optimization to ensure that by the switching point the design space has been widely explored – this is the defined function of MOGA in such a multi-fidelity optimization. The hybrid optimization using the low- and high-fidelity models showed that the operating efficiency of the submarine components may be increased by appropriate sizing and design within a computationally affordable optimization framework.

REFERENCES

[1] B. A. Skinner, G. T. Parks, and P. R. Palmer "Comparison of Submarine Drive Topologies Using Multiobjective Genetic Algorithms" IEEE Transactions on Vehicular Technology, vol. 58, pp. 57-68, 2009.

[2] Z. Zhou, Y. S. Ong, P. B. Nair, A. J. Keane, and K. Y. Lum, "Combining Global and Local Surrogate Models to Accelerate Evolutionary Optimization," IEEE Transactions on Systems, Man and Cybernetics, Part C: Applications and Reviews, vol. 37, pp. 66-76, 2007.

[3] N. M. Alexandrov, "Variable-fidelity Models in Optimization of Simulation-based Systems," presented at Department of Aeronautics, University of Rome, Rome, March 2002.

[4] T. D. Robinson, M. S. Eldred, K. E. Willcox, and R. Haimes, "Strategies for Multifidelity Optimization with Variable Dimensional Hierarchical Models," presented at 47th AIAA/ASME/ASCE/AHS/ASC Structures, Structural Dynamics, and Materials Conference, Newport, RI, USA, 2006.

[5] S. Choi, J. J. Alonso, and I. M. Kroo, "Multi-fidelity Design Optimization of Lowboom Supersonic Business Jets," presented at 10th AIAA/ISSMO Multidisciplinary Analysis and Optimization Conference, Albany, NY, USA, 2004.

[6] M. G. Hutchinson, E. R. Unger, W. H. Mason, B. Grossman, and R. T. Haftka, "Variable-complexity Aerodynamic Optimization of High-speed Civil Transport Wing," Journal of Aircraft, vol. 31, pp. 110-116, 1994.

[7] L. A. Schmitt and H. Miura, "Some Approximation Concepts for Structural Synthesis," AIAA Journal, vol. 12, pp. 692-699, 1974.

[8] J.-F. M. Barthelemy and R. T. Haftka, "Approximation Concepts for Optimum Structural Design – a Review," Structural and Multidisciplinary Optimization, vol. 5, pp. 129-144, 1993.

[9] G. M. Rodriguez, J. E. Renaud, and V. Tomar, "A Variable Fidelity Model Management Framework for Designing Multiphase Materials," ASME Journal of Mechanical Design, vol. 130, pp. 091702-1-13, 2008.

[10] R. T. Haftka, "Combining Local and Global Approximations," AIAA Journal, vol. 29, pp. 1523-1525, 1991.

[11] D. Huang, T. Allen, W. Notz, and R. Miller, "Sequential Kriging Optimization Using Multiple-fidelity Evaluations," Structural and Multidisciplinary Optimization, vol. 32, pp. 369-382, 2006.

[12] S. E. Gano, J. E. Renaud, and B. Sanders, "Hybrid Variable Fidelity Optimization Using a Kriging-based Scaling Function," AIAA Journal, vol. 43, pp. 2422-2430, 2005.

[13] H. S. Kim, M. Koo, and J. Ni, "A Hybrid Multi-fidelity Approach to the Optimal Design of Warm Forming Processes Using a Knowledge-based Artificial Neural Network," International Journal of Machine Tools and Manufacture, vol. 47, pp. 211-222, 2007.

[14] M. Molinari, "Reduced Order Modelling for Turbomachinery," Ph.D. thesis, Department of Engineering, University of Cambridge, Cambridge, UK, 2010.

[15] N. M. Alexandrov and R. M. Lewis, "Outstanding Issues in Simulation-based Design Optimization," presented at SIAM Conference on Computational Science and Engineering, San Diego, CA, USA, 2003.

[16] C. M. Fonseca and P. J. Fleming, "Multiobjective Optimization and Multiple Constraint Handling with Evolutionary Algorithms. I. A Unified Formulation," IEEE Transactions on Systems, Man and Cybernetics Part A: Systems and Humans, vol. 28, pp. 26-37, 1998.

[17] D. M. Jaeggi, G. T. Parks, T. Kipouros, and P. J. Clarkson, "The Development of a Multi-objective Tabu Search Algorithm for Continuous Optimisation Problems," European Journal of Operational Research, vol. 185, pp. 1192-1212, 2006.

[18] R. Hooke and T. A. Jeeves, "Direct Search Solution of Numerical and Statistical Problems," Journal of the Association for Computing Machinery, vol. 2, pp. 212-229, 1961.

[19] M. M. Bernitsas, D. Ray, and P. Kinley, "KT, KQ and Efficiency Curves for the Wageningen B-series Propellers," University of Michigan, Department of Naval Architecture and Marine Engineering, Publication No. 240, 1981.

[20] Converteam, "Cambridge University - Converteam confidentiality agreement," 2007.

[21] E. Zitzler, L. Thiele, M. Laumanns, C.M. Fonseca, and V. G. da Fonseca, "Performance Assessment of Multiobjective Optimizers: An Analysis and Review." IEEE Transactions on Evolutionary Computation, vol. 7, pp. 117-132. 2003